A NON-CONSUMABLE METAL ANODE FOR PRODUCTION OF ALUMINUM WITH LOW-TEMPERATURE FLUORIDE MELTS

Theodore R. Beck
Electrochemical Technology Corp.
1601 Dexter Avenue North
Seattle, Washington 98109

ABSTRACT

A dimensionally-stable alloy anode is being developed to operate in the eutectic $NaF-AlF_3$ bath at about 750°C as described in Light Metals 1994. A small range of composition of Cu-Ni-Fe alloy appears to have satisfactory low anodic oxidation rate and high oxide conductivity. The anodic oxidation rate is similar to air oxidation rate at the same temperature. Air oxidation studies carried out to 6 months appear to have satisfactory low rates. Operation with multiple, vertical, monopolar, metal anodes and TiB_2 plate cathodes at 0.5 A/cm² each side promises a 20-fold decrease in cell volume compared to conventional H-H cells, and a specific energy consumption of 11 kWh/kg.

INTRODUCTION

Hall in his first issued patent in 1889 (1) mentions the use of a copper anode in a cryolite bath, but the oxidation rate was too high and the industry went down the path of the consumable carbon anode. Many attempts have been made to find a substitute non-consumable anode (2) but to date none have reached commercial success. The closest to success has been the Alcoa nickel ferrite - copper cermet (3) but after more than ten years of testing it in cryolite baths at conventional operating temperature of about 950°C success is still elusive.

The present paper describes laboratory evaluations of a copper-nickel-iron alloy (4) in a low temperature $NaF-AlF_3$ bath operating at about 750°C. The more oxidation-resistant alloy compared to copper combined with the gentler conditions show promise as a viable, lower-cost alternative to the conventional Hall-Heroult process. Operation of the low-temperature bath was described in Light Metals 1994 (5). Sadoway (6) has discussed criteria for use of metal alloy anodes, although he reported on different alloys.

ALLOY ANODE

Although there are no known commercial alloys in the region optimum for an anode in the Cu:Ni:Fe triangular diagram, this system has been studied for it's scientific interest (7,8). A single solid-phase region exists near the Ni apex, but other compositions tend to split into two phases on cooling. Rapid cooling from the melt is desirable, but there is a region of compositions encompassing the anode optimum that can be homogenized by appropriate heat treatment.

Most of the alloy anodes tested were made by sintering mixtures of high-purity powders at about 1180°C in argon atmosphere in a Globar heated furnace. These were 50 mm in diameter and about 3 mm thick. Smaller button anodes, used for screening the effects of low-concentration metal additives on oxidation rate, were melted in graphite crucibles in a nitrogen atmosphere at about 1400°C.

Oxidation Rate

Oxidation rates of anode alloys were measured in air at 800°C and at 750°C in the cell described in Ref. (5). Weight gain per unit exposed area for several types of specimens and conditions is shown as a function of time in Fig. 1. The dashed line is average literature data (9,10) for copper in oxygen. Copper as an anode in fluoride melts is surprisingly close to the literature O_2 oxidation data. Alloy of Cu70:Ni15:Fe15 composition produced from a melt has a lower oxidation rate but sintered alloy is near that of copper, probably because of internal oxidation through the pores. Sintered alloy as an anode operated at 0.5 A/cm² is close to the same line for the alloy cooled from the melt, although there is some scatter in the data. Apparently the internal pores become plugged with molten salt and slow the internal oxidation. Nearly all of the anode tests were of seven hours duration. Interestingly, a later test run for 100 hours at 0.1 A/cm² gave an extremely low amount of oxidation. This test was run after a precise method was developed for control of AlF_3 concentration in the bath.

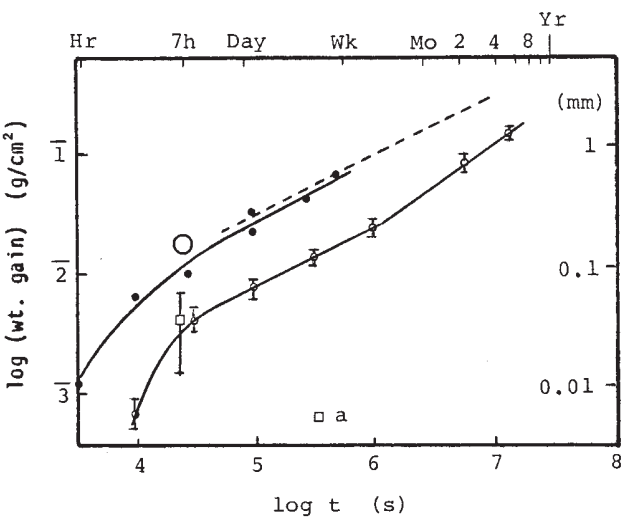

Fig. 1: Comparison of amount of air-oxidation weight gain of Cu70:Ni15:Fe15 alloy and copper to equivalent weight gain of alloy anode; scale at right is equivalent depth of alloy oxidized in mm
--- Cu in oxygen at 800°C, Ref. (9,10)
o Cu anode in cell at 750°C
• Alloy sintered at 1150°C, in air at 800°C
Φ Alloy melted at 1400°C, in air at 800°C
□ 1150°C sintered anodes, in cell at 750°C
a, is a 100-hr run at 0.1 A/cm2 and 750°C, Fig. 4

Each kind of test gave a different index representing the amount of oxidation. The air oxidation test gave weight gain of oxygen in the oxide. Weight gain was not an appropriate measurement for the cell oxidation tests because of bath contamination. A weight loss of metal after chipping off the oxide was used as measurement. Weight loss correlated well with thickness of oxide measured on oxide chips under the microscope. A factor of 0.126 for average alloy composition was used to convert from metal weight loss to oxygen weight gain. A factor of 0.890 converted weight gain in g/cm^2 to alloy thickness lost in cm.

Oxidation of copper in oxygen and in air follows the quadratic oxidation law (10)

$$\ell^2 = K t \qquad (1)$$

in which ℓ is the thickness of metal oxidized, K is a rate constant and t is time. The rate constant, K, is shown as a function of temperature in the Arrhenius plot of Fig. 2. The solid circles are literature data (9,10) for oxidation in oxygen. The triangles for oxidation in air, measured in the present work, fell on the same line, consistent with oxide growth limited by solid state diffusion. Oxidation rate of copper as an anode is only slightly above the gaseous oxidation rate line. The oxidation rate constant of the Cu70:Ni15:Fe15 alloy anode is about an order of magnitude below the copper line.

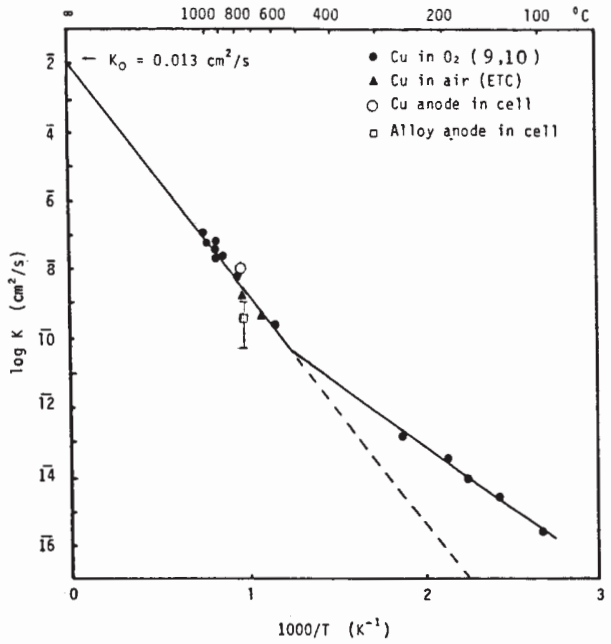

Fig. 2: Arrhenius plot for copper oxidation rate constant in Equation 1.

Average anode oxidation rate in a seven hour run is very sensitive to AlF_3 composition of the bath as shown in Fig. 3. Below 42 mol% AlF_3 the anode suffers a catastrophic blister corrosion. At about the same concentration, coincidently, crylolite deposits on the cathode (5). At higher than 46 mol% AlF_3 a high resistance develops on the anode due to AlF_3 precipitation on it. The operating range of 42 to 46 mol% AlF_3 is narrow, but a rapid, simple, accurate and inexpensive method was developed to control it toward the end of the experimental program. An example of the close control of AlF_3 concentration in a 100-hour run at 0.1 A/cm^2 is shown in Fig. 4. Bath additions were enriched in AlF_3. It is probable that anode oxidation rates would have been lower in Fig. 3 if better control of bath composition had been available earlier in the program.

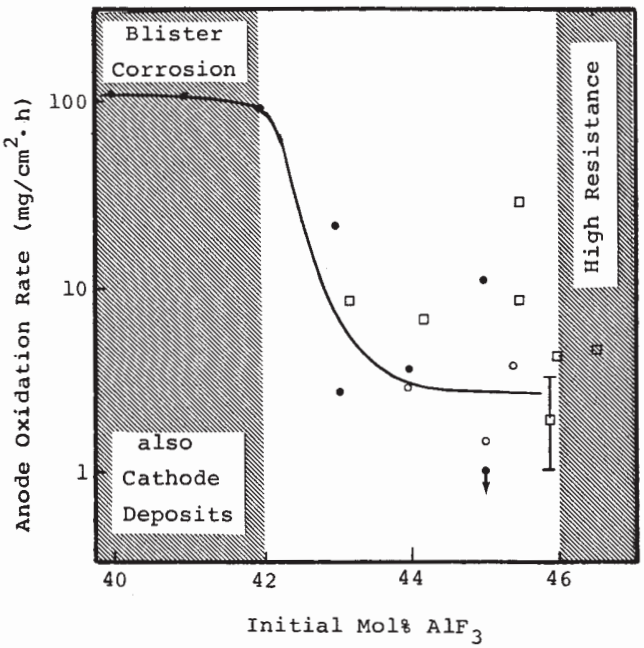

Fig. 3: Average anode oxidation rate in 7 hours by weight loss as a function of mol% AlF_3

Cu70:Ni15:Fe15	•	NaF-AlF_3
	□	NaF-KF-LiF-AlF_3
Cu50:Ni37:Fe13	○	NaF-AlF_3

A window of operability also exists in respect to alloy composition as shown in Fig. 5, which was obtained from runs made with optimum initial bath composition, 44 ± 1 mol% AlF_3. Isooxidation rate lines are shown for 1 and 5 mg/cm^2·h at 7 hours. The minimum oxidation rate appears at about Cu55:Ni35:Fe10. A region of high electrical resitance of the anode oxide exists below about 12% Fe (region A) in the area of minimum oxidation rate. The reason is not understood yet. For that matter, the reason for electronic conductivity of the oxide above region A is not known as the flow of electrons is opposite to that in a copper oxide rectifier. Metal compositions in region B in Fig. 5 are subject to blister corrosion. Coincidently, compositions in region B cannot be homogenized by heat treatment. Alloys with low copper tend to be brittle. The optimum anode composition appears to be about Cu60:Ni25:Fe15.

Aluminum Purity and Oxide Dissolution Rate

Aluminum metal produced in a non-consumable anode cell must meet a certain level of purity. The criterion considered here is that Cu, Ni and Fe should each individually be less than 0.03 wt%. Although a 10 A cell is not an ideal test vehicle, a series of tests indicated that the required purity can be achieved.

A series of 7-hour tests was run using a single Cu70:Ni15:Fe15 anode to determine aluminum contamination versus time. The anode oxide was not stripped from the anode between tests. A fresh bath mixture was used in each successive run. The metal produced in each run was analyzed for Cu and Ni by an outside laboratory using an optical emission spectrograph calibrated to Alcoa standards. Iron concentrations were below the detection limit of 0.12%. Copper and nickel concentrations, plotted as a function of anode electrolysis time in Fig. 6, show a decline with time. Nickel concentrations were all below the target maximum level of 0.03 wt%, while the Cu concentrations were rapidly approaching the target. The tests were severe in that the anodes were subject to thermal shock on cooling to room temperature between runs and to reheating to operating temperature. Had the aluminum

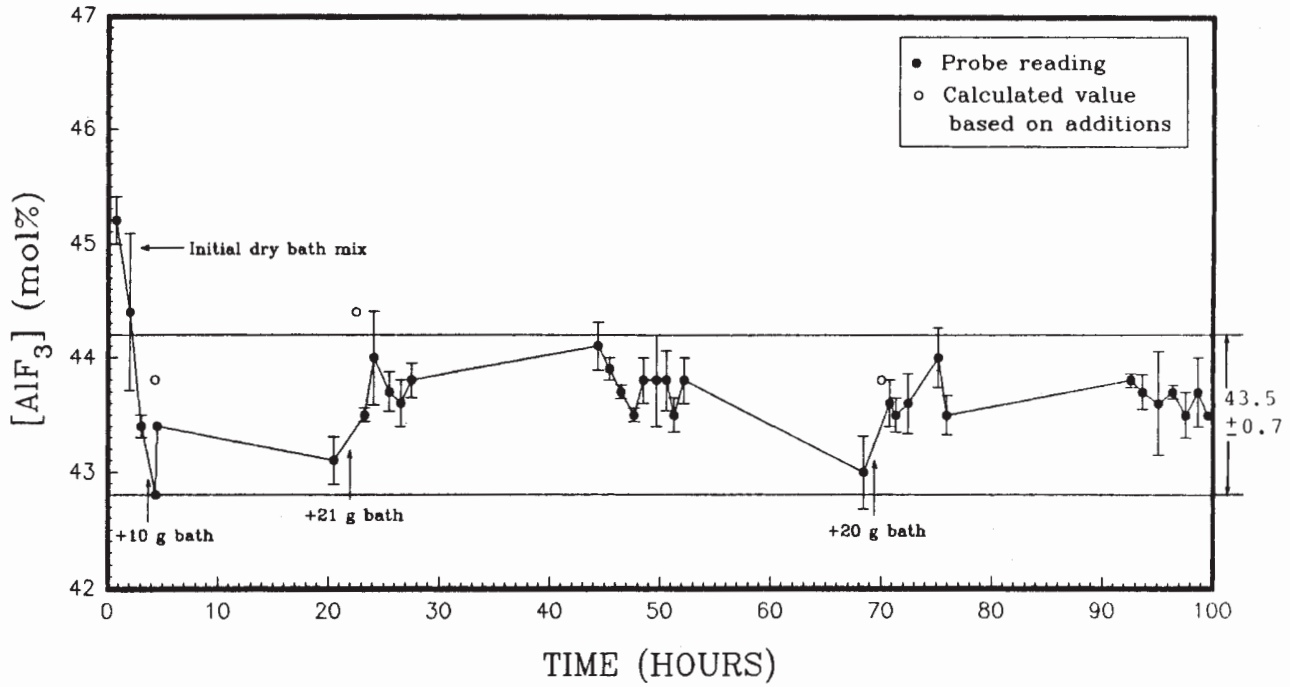

Fig 4: Plot of AlF_3 concentration for 100-hour run at 0.1 A/cm^2.

current efficiencies been greater than 50% the Cu and Ni concentrations would also have been lower. Average data for five other 7-hour runs selected at ramdom are consistent with the series as seen in Fig. 6. The initial high-Cu (0.3%) aluminum produced could be used for aircraft alloys.

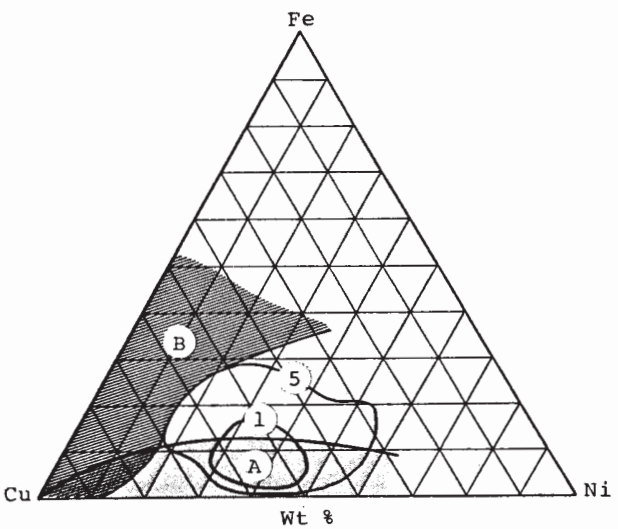

Fig. 5: Isooxidation rate lines for alloy anodes at 1 and 5 mg/cm^2·h average at 7 hours using initial 44 ± 1 mol% AlF_3 electrolyte; stipled region A has high oxide resistance; region B exhibited blister corrosion.

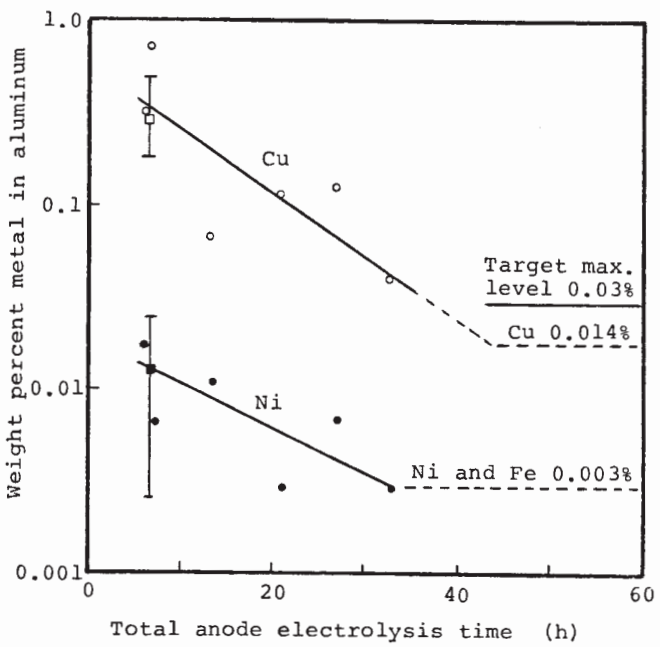

Fig. 6: Decrease in Cu and Ni contamination in aluminum produced versus anode electrolysis time.
□ ▪ Average of five runs

A first approximation can be made for the limiting Cu, Ni and Fe concentrations at long time by mass transfer considerations. It has been shown that dissolution rate of a cermet anode was mass transport controlled into the bath (3). The oxide skin on the alloy anodes is assumed to behave similarly. Of the

oxides of the three metals, NiO has the lowest solubility (3). It may be conservatively assumed that Ni had reached its minimum steady state level of 0.003 wt% at 33 hours in Fig. 6. The steady state concentrations of Cu and Fe would then be in their relative proportions in the metal of (0.003)(70/15) =0.014% and (0.003)(15/15) = 0.003% respectively. These extrapolations are shown in Fig. 6. For a current efficiency closer to 100% than 50% these metal contamination values would all be halved.

The cumulative amount of Cu dissolved from the anode was calculated from the Cu analyses in Fig. 6 and the amount of aluminum produced in each 7-hour period of operation. The equivalent alloy thickness to the Cu dissolved as a function of time in seconds is

$$\ell_m^d = 2.6 \times 10^{-5}\, t^{0.42} \quad (mm) \qquad (2)$$

This equation is only valid up to the time when the three alloy constituents dissolve in their ratio in the metal or at about 44 hours when Cu reaches its terminal concentration by the assumptions in Fig. 6. Thereafter the dissolution rate would be linear in time.

Projected Long-Term Anode Performance

A projection of long-term performance of an anode is useful for planning future tests for development of the technology. The projected performance is based on extrapolations of oxide growth rate and the oxide dissolution rate and is shown in Fig. 7. The oxidation depth of the alloy anode is initially controlling and is described by the equation

$$\ell_m^{ox} = 1.4 \times 10^{-5}\, t^{0.6} \quad (mm) \qquad (3)$$

An alloy like Cu65:Ni25:Fe25 oxidizes as time to the 0.6 power. Likewise Pilling and Bedworth (11) found that binary Cu:Ni alloys oxidized with an exponent greater than 0.5 at compositions between 20 and 70% copper. Equation 3 was drawn through the lower part of the error bar in Fig. 1 because it was assumed that average performance would be improved with better control of bath composition (Fig. 4). The initial oxide dissolution rate is controlled by Eq. 2, but the rate is assumed to become linear at a time of about 45 hours as indicated in Fig. 6 for Cu. The linear rate beginning at a time of 45 hours has the equation

$$\ell_m^d = 3 \times 10^{-8}\, t \quad (mm) \qquad (4)$$

which is plotted in Fig. 7. The actual alloy oxidation depth should asymptotically approach Eq. 3 at short time and Eq. 4 at long times, with curvature in between. It is seen that a time of several months is required to reach the dissolution rate limit by this model.

The net thickness of oxide is determined by the difference in oxidation and dissolution rates. The oxide thickness formed or dissolved is 1.67 times the equivalent metal oxidation depth. Solutions to the equations, with and without dissolution, are shown in Fig. 8. According to this model and the parameters used, the asymptotic oxide thickness at long time is about 0.1 mm. The next phase of the technology development will include experimental testing of these models.

300 AMPERE CELL

A 300 ampere cell was designed and built to obtain a more realistic evaluation of the technology. The initial design was based on the MacMullin concept (12) of "scale down by dissection" of a proposed full-scle commercial cell design. That is, the critical dimension of electrode height is preserved and a short horizontal length of electrode is used. The electrode height is the most important factor in determining the bath

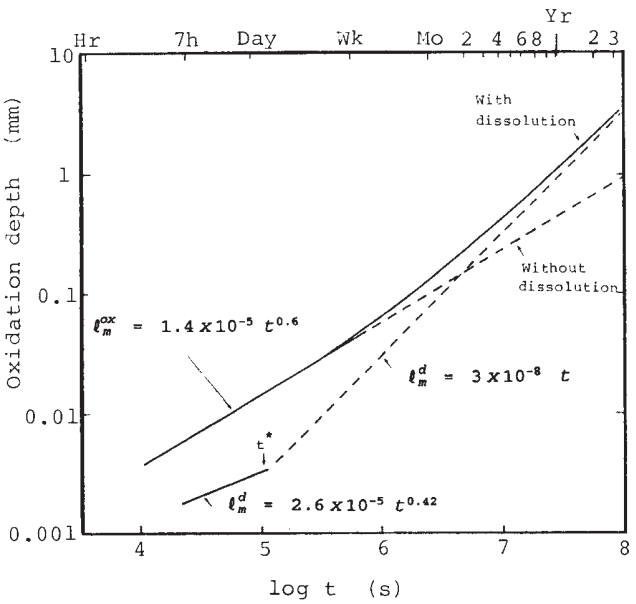

Fig. 7: Projected metal oxidation depth with oxide dissolution.

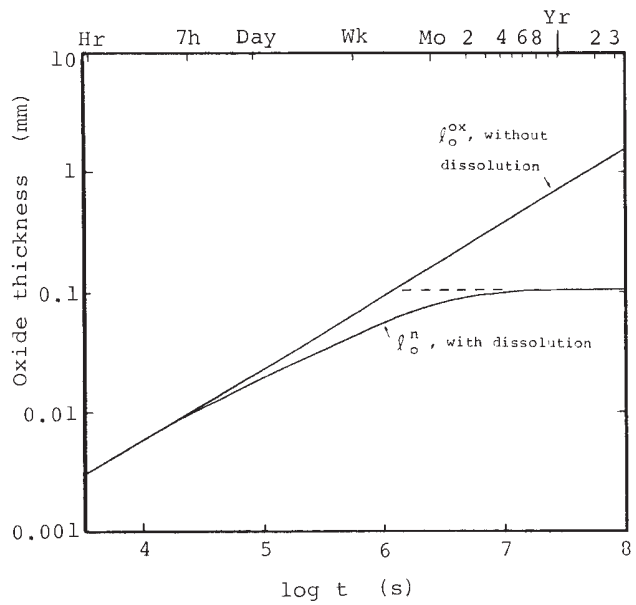

Fig. 8: Projected oxide thickness as a function of time.

circulation rate by oxygen bubbles evolved at the anode, and the consequent mass transfer rate at the anode and maintenance of suspension of the Al_2O_3 particles (5). Other factors intended to be evaluated were, an alloy anode liner concept, and continuous aluminum removal from the cell cavity.

A compromise was made in the first cell design because of the high cost of specially-made TiB_2 cathode sizes. Great Lakes Research had off-the-shelf TiB_2-graphite tiles that were 4 in. x 6 in. x 1/2 in. that were relatively inexpensive compared to the initially-proposed 6 in. x 10 in. x 1/2 in. cathode that required new tooling. It was decided to use two such smaller cathode tiles with a Cu:Ni:Fe alloy anode plate between them to obtain the proposed 300 A capacity. The scale-down by dissection principle was compromised, but it was considered that sufficient gas lift would still be achieved to prevent settling of alumina particles.

The cell that was built, consisted of a cast metal anode vessel, Fig. 9, in a firebrick insulated steel shell. Alloy for the anode vessel and anodes was induction melted and cast in sand molds at a Seattle foundry. The vessel as a cell was heated by ac heating elements on its four outside vertical faces. Two titanium diboride cathodes 4 in. x 6 in. x 1/2 in. were immersed in the electrolyte, with a 4 in. x 6 in. x 1/4 in. alloy anode in between them, Fig 10. The anode-cathode spacing was 1/2-inch. Stainless steel straps conducted current to the electrodes. The bottom of the cell was sloped so that aluminum formed would collect at one end for removal.

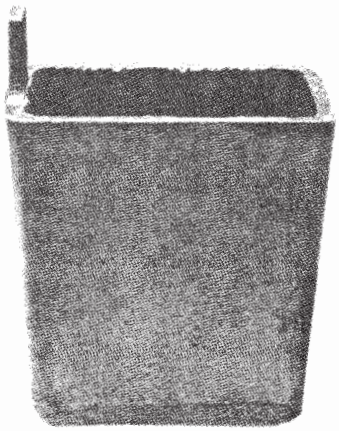

Fig. 9: Photograph of anode vessel.

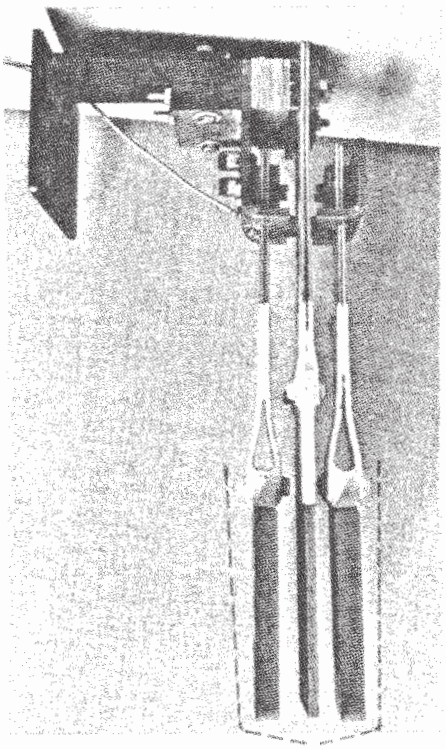

Fig. 10: Photograph of TiB_2 cathode and alloy anode assembly; dashed line is outline of inside of anode vessel.

A view of the assembled cell in Fig. 11 shows the insulating firebrick around the anode vessel and a fused alumina thermocouple tube for continuous temperature measurement. The bottom of the fume hood is seen.

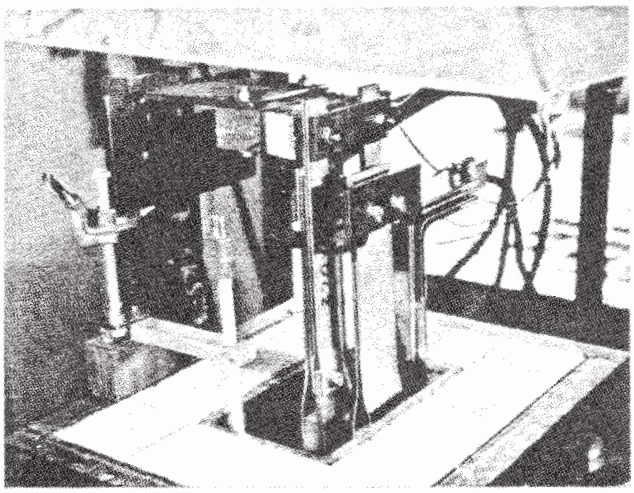

Fig. 11: Photograph of assembled cell.

One preliminary test run of the 300 A cell was made. The electrolyte composition was the eutectic 44 mol% AlF_3, 56 mol% NaF. Heatup to operating temperature of 750°C and complete melting of electrolyte took five hours. Two hours of electrolysis at 300 amperes followed. Cell voltage was constant at 3.5 volts. A polarization curve for the cell in Fig. 12 shows that the voltage extrapolates to about 2.3 V, the thermodynamic potential, at zero current. The preliminary testing was not long enough to obtain current efficiency data for this cell. Funding was not sufficient for further runs. The average current density was about 0.5 A/cm^2 on each side of the two sides of the anode and cathodes, corresponding to a current density of 1 A/cm^2 for a single side of anodes and cathodes in a conventional Hall-Herault cell.

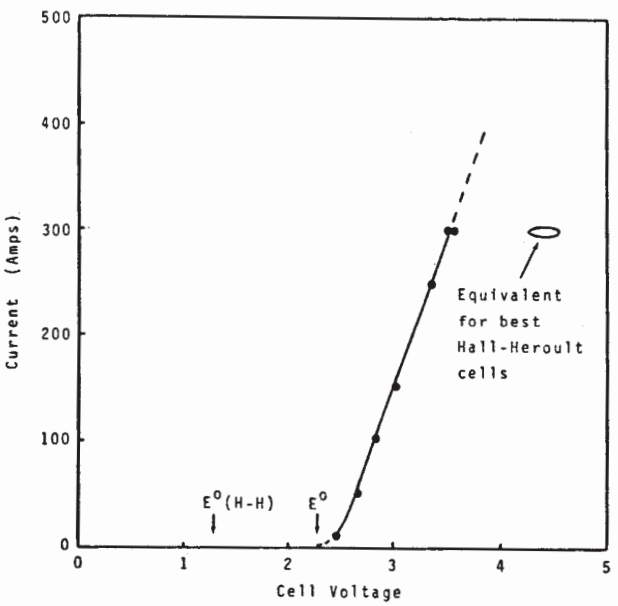

Fig. 12: Current-voltage curve for 300 A cell.

PROJETED ENERGY EFFICIENCY

A projected specific energy consumption for a full scale cell can be made from estimated cell voltage and current efficiency. A cell voltage of 3.5 V at 0.5 A/cm2 should be achievable in a commercial cell as in the 300 A cell. Current efficiency for a commercial cell is estimated by extrapolation of the correlation of laboratory cell data (5). Current efficiency was related to the ratio of cell current to surface area of the aluminum balls dripping off the TiB_2 cathodes and collected at the aluminum removal end of the cell. The relation found (5)

$$\% CE = 100 - \frac{40}{I/S} \qquad (5)$$

is plotted in Fig. 13. Assuming a 200,000 A cell and a surface area of aluminum balls of 2000 cm2 gives I/S = 100 and a 99% current efficiency in Fig. 13. Equation 5 needs to be verified in larger cells, but a current efficiency of 99% and a cell voltage of 3.5 V gives about 11 kWh/kg.

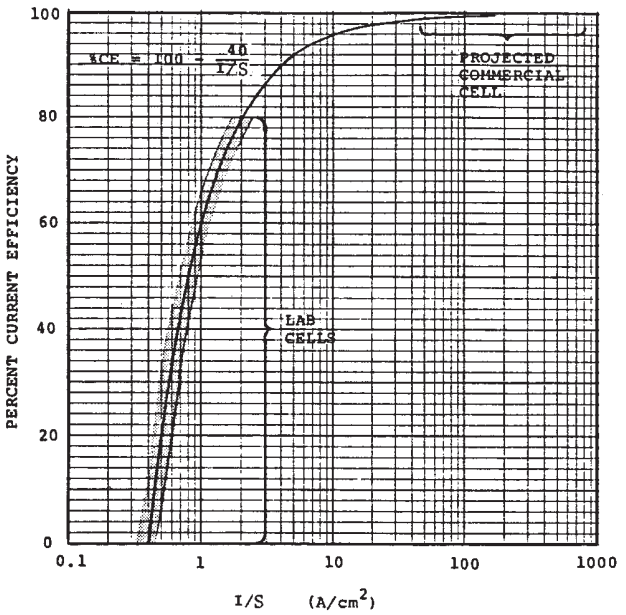

Fig. 13: Correlation of current efficiency with ratio of cell current to total surface of aluminum balls in cell (5).

CONCLUSIONS

1. An alloy of Cu:Ni:Fe was shown to have promise as a non-consumable anode in a low-temperature, 750°C, bath for manufacture of aluminum.

2. Composition of AlF3:NaF electrolyte is critical but it can be readily controlled.

3. Aluminum purity meets criterion of < 0.03% Cu, Ni, or Fe after about two days after startup; initial high, 0.3% Cu, could be used in alloys.

4. A specific energy consumption of 11 kWh/kg appears feasible in a commercial cell using the non-consumable alloy anodes.

ACKNOWLEGDMENT

The author acknowledges the contributions of Richard J. Brooks of Brooks Rand, Ltd., who collaborated on the process development, and of Prof. Jomar Thonstad of the Institute of Technical Electrochemistry in Trondheim who consulted on the scientific aspects. The work was supported by National Science Foundation SBIR Phase I and II Grants and a U.S. Department of Energy, Energy Related Inventions Program Grant.

REFERENCES

1. C. M. Hall, U.S. Patent No. 400,664, Process of Reducing Aluminum from Its Fluoride Salts by Electrolysis, April 2, 1889

2. K. Billehaug and H.A. Øye, "Inert Anodes for Aluminum Electrolysis in Hall-Heroult Cells," Aluminium, 57 (1981), 146-150 and 228-231.

3. Alcoa Final Report, "Inert Anodes for Aluminum Smelting," DOE Contract DOE/CS/40158-20, February, 1986.

4. T. R. Beck and R. J. Brooks, U. S. Patent No. 5,284,562, Non-Consumable Anode and Lining for Aluminum Electrolytic Reduction Cell, Feb. 8, 1994

5. T. R. Beck, Production of Aluminum with Low Temperature Melts, Light Metals 1994, TMS Warrendale, PA, 417

6. D. R. Sadoway, A Materials Systems Approach to Selection of Nonconsumable Anodes for the Hall Cell, Light Metals 1990, TMS Warrendale, PA, 403; J. N. Hryn and D. R. Sadoway, Cell Testing of Metal Anodes for Aluminum Electrolysis, Light Metals 1993. TMS Warrendale, PA, 475

7. E. P. Butler and G. Thomas, Structure and Properties of Spinodally Decomposed Cu-Ni-Fe Alloys, Acta Met., 18,(1970), 347

8. P. Spencer, et al, Calculation of the FCC/Liquid Phase Equilibria in the Cu-Ni-Fe System, CALPHAD, 9, (1985), 191

9. K. Hauffe, Oxidation of Metals, Plenum Press, New York, 1965

10. P. Kofstad, High Temperature Corrosion, Elsevier Applied Science, New York, 1988

11. N. B. Pilling and R. E. Bedworth, Oxidation of Copper-Nickel Alloys at High Temperatures, Ind. Eng. Chem., 17, (1925), 372

12. R.B. MacMullin, "The Problem of Scale-Up in Electrolytic Processes," Electrochemical Technology, 1, (1963), 5